Some Basic Characteristics of Broadband Negative Resistance Oscillator Circuits

By K. KUROKAWA

(Manuscript received January 14, 1969)

This paper discusses the behavior of oscillators with multiple-resonant circuits. It discusses the condition for free-running stable oscillations, the injection locking phenomena, the stable locking range, the noise of free-running and injection-locked oscillators, and a condition for parasitic oscillations in detail, and presents a graphical interpretation of this study for clarity. Finally, this paper shows how broadbanding of oscillators can be achieved with a double-resonant circuit. This provides a systematic guide for the design of broadband frequency deviators and broadband injection-locked oscillators for numerous applications.

I. INTRODUCTION

With the advent of high-frequency negative resistance elements such as tunnel diodes, Gunn diodes, and IMPATT's, it now appears practical, at microwave frequencies, to build negative resistance oscillators which perform various functions other than that of a fixed frequency oscillator.[1] Among the proposals recently made are variable frequency oscillators as FM deviators, and locked oscillators as FM amplifiers, limiters, and FM demodulators.[2-4] In the past, the analysis of these oscillators was primarily based on a simple model with a single-resonant circuit.[5-8] In practice, however, the designer of such a microwave circuit provides a number of tuning elements and adjusts them by trial and error until a desired bandwidth of locking or frequency deviation is obtained. During this adjustment, the designer observes numerous phenomena, including sudden changes in noise or oscillating frequency, as well as various hysteresis effects which could not be explained by the simple oscillator model.

This paper presents a more realistic model of oscillators in which the load is separated from the active device by a multiple-resonant circuit. This gives us a better understanding of the oscillator behavior and, hopefully, a more systematic approach toward an oscillator design for broadband applications.

II. EQUATIONS FOR AMPLITUDE AND PHASE OF OSCILLATING CURRENT

Consider the circuit shown in Fig. 1. The active device is represented by $-\bar{R} + j\bar{X}$ and the load by Z_L. The box between the active device and the load represents a multiple-resonant circuit; $Z(\omega)$ is the impedance looking into the box from the active device. As far as the active device is concerned, the entire circuit can be expressed as a series connection of $Z(\omega)$ and $-\bar{R} + j\bar{X}$, as shown in Fig. 2 where $e(t)$ represents noise or locking signal voltages that may be present. Let the current flowing through the active device be

$$i(t) = A \cos (\omega t + \varphi), \tag{1}$$

where A and φ are assumed to be slowly varying functions of time. From the beginning, the effects of higher harmonics are neglected since they disappear in the process of averaging over one period of the oscillation which we perform later.[7,8] The voltage drop across the active devices is given by

$$v = -\bar{R}A \cos (\omega t + \varphi) - \bar{X}A \sin (\omega t + \varphi) \tag{2}$$

where $\bar{R}$ and $\bar{X}$ are functions of the current amplitude A. In the following discussion the frequency dependence of $\bar{R}$ and $\bar{X}$ are neglected, which is generally justifiable over the frequency range of interest. Furthermore, the magnitude of $\bar{X}$ is assumed to be small, which is usually justifiable after lumping any large constant portion of the device reactance in with $Z(\omega)$.

In order to calculate the voltage drop across $Z(\omega)$, consider the time derivative of $i(t)$. The first derivative is given by

$$\frac{di}{dt} = -A\left(\omega + \frac{d\varphi}{dt}\right) \sin (\omega t + \varphi) + \frac{dA}{dt} \cos (\omega t + \varphi)$$

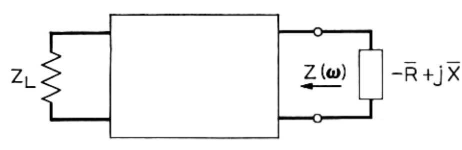

Fig. 1 — Schematic diagram for an oscillator.

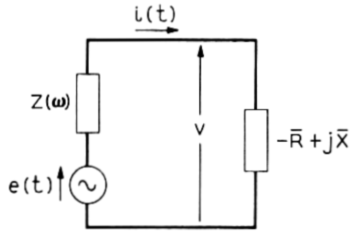

Fig. 2 — An equivalent circuit of the oscillator in Fig. 1.

$$= \mathrm{Re}\left\{\left[j\left(\omega + \frac{d\varphi}{dt}\right) + \frac{1}{A}\frac{dA}{dt}\right]Ae^{j(\omega t+\varphi)}\right\}.$$

Similarly, to first order approximation, the nth derivative is given by

$$\frac{d^n i}{dt^n} \cong \mathrm{Re}\left\{\left[j\left(\omega + \frac{d\varphi}{dt}\right) + \frac{1}{A}\frac{dA}{dt}\right]^n Ae^{j(\omega t+\varphi)}\right\}.$$

In ac circuit theory, the time derivative corresponds to multiplication by $j\omega$. Therefore, replacing ω by $\omega + d\varphi/dt - j(1/A)(dA/dt)$ everywhere in $Z(\omega)$, Re $\{ZI\}$ should give the desired voltage drop, where I is the expression for $i(t)$ in the form of $Ae^{j(\omega t+\varphi)}$. Assuming $d\varphi/dt \ll \omega$ and $(1/A)(dA/dt) \ll \omega$, we have

$$\begin{aligned} Z\left(\omega + \frac{d\varphi}{dt} - j\frac{1}{A}\frac{dA}{dt}\right) &\cong Z(\omega) + \frac{dZ(\omega)}{d\omega}\left(\frac{d\varphi}{dt} - j\frac{1}{A}\frac{dA}{dt}\right) \\ &= R(\omega) + jX(\omega) + [R'(\omega) + jX'(\omega)]\left(\frac{d\varphi}{dt} - j\frac{1}{A}\frac{dA}{dt}\right) \end{aligned} \tag{3}$$

where $R(\omega) = \mathrm{Re}\,[Z(\omega)]$, $X(\omega) = \mathrm{Im}\,[Z(\omega)]$, and the primes indicate the derivatives with respect to ω. Using the above approximate expression, Re $\{ZI\}$ is calculated to be

$$\begin{aligned} \mathrm{Re}\,\{ZI\} = &\left[R(\omega) + R'(\omega)\frac{d\varphi}{dt} + X'(\omega)\frac{1}{A}\frac{dA}{dt}\right]A\cos(\omega t + \varphi) \\ &- \left[X(\omega) + X'(\omega)\frac{d\varphi}{dt} - R'(\omega)\frac{1}{A}\frac{dA}{dt}\right]A\sin(\omega t + \varphi). \end{aligned}$$

Referring to Fig. 2, we have $v + \mathrm{Re}\,\{ZI\} = e(t)$ which is equivalent to

$$\left[R(\omega) - \bar{R} + R'(\omega)\frac{d\varphi}{dt} + X'(\omega)\frac{1}{A}\frac{dA}{dt}\right]A\cos(\omega t + \varphi)$$

$$- \left[X(\omega) + \bar{X} + X'(\omega)\frac{d\varphi}{dt} - R'(\omega)\frac{1}{A}\frac{dA}{dt}\right]A\sin(\omega t + \varphi) = e(t).$$

After multiplying this equation by $\cos(\omega t + \varphi)$ and $\sin(\omega t + \varphi)$, respectively and integrating over one period of oscillation, we obtain

$$R(\omega) - \bar{R} + R'(\omega)\frac{d\varphi}{dt} + X'(\omega)\frac{1}{A}\frac{dA}{dt} = \frac{1}{A}e_c(t) \tag{4}$$

$$-X(\omega) - \bar{X} - X'(\omega)\frac{d\varphi}{dt} + R'(\omega)\frac{1}{A}\frac{dA}{dt} = \frac{1}{A}e_s(t) \tag{5}$$

where

$$e_c(t) = \frac{2}{T_o}\int_{t-T_o}^{t} e(t)\cos(\omega t + \varphi)\,dt \tag{6}$$

$$e_s(t) = \frac{2}{T_o}\int_{t-T_o}^{t} e(t)\sin(\omega t + \varphi)\,dt \tag{7}$$

and T_o is the oscillation period. Equations (4) and (5) both contain $d\varphi/dt$ and dA/dt. However, by multiplying equation (4) by $X'(\omega)$ and equation (5) by $R'(\omega)$ and adding, an equation with dA/dt alone is obtained. Similarly, multiplying equation (4) by $R'(\omega)$ and equation (5) by $-X'(\omega)$ and adding, gives an equation with $d\varphi/dt$ alone. These are

$$[R(\omega) - \bar{R}]X'(\omega) - [X(\omega) + \bar{X}]R'(\omega) + |\,Z'(\omega)\,|^2\frac{1}{A}\frac{dA}{dt}$$

$$= \frac{1}{A}[X'(\omega)e_c(t) + R'(\omega)e_s(t)] \tag{8}$$

$$[R(\omega) - \bar{R}]R'(\omega) + [X(\omega) + \bar{X}]X'(\omega) + |\,Z'(\omega)\,|^2\frac{d\varphi}{dt}$$

$$= \frac{1}{A}[R'(\omega)e_c(t) - X'(\omega)e_s(t)]. \tag{9}$$

Equations (8) and (9) are the basic equations for the amplitude and phase of an oscillating current.

For a steady-state free-running oscillation, we assume $e_c(t) = e_s(t) = 0$, $dA/dt = 0$ and $d\varphi/dt = 0$. Thus, from equations (8) and (9) we have

$$R(\omega) - \bar{R} = 0, \quad X(\omega) + \bar{X} = 0 \tag{10}$$

which determine the amplitude A_o and the frequency ω_o of the oscillation. Suppose A somehow deviates from its steady-state value A_o by a small amount δA. We then have

$$R(\omega_o) - \bar{R} = \frac{\delta A}{A_o} sR_o\,, \qquad X(\omega_o) + \bar{X} = \frac{\delta A}{A_o} rR_o \tag{11}$$

where R_o indicates the value of $\bar{R}$ at $A = A_o$ [which is also equal to $R(\omega_o)$], and sR_o and rR_o represent $A_o(-\partial\bar{R}/\partial A)$ and $A_o(\partial\bar{X}/dA)$, respectively, as indicated in Fig. 3.

From equations (8) and (11), we obtain a differential equation for δA. To first-order approximation, it is

$$sR_oX'(\omega_o)\frac{\delta A}{A_o} - rR_oR'(\omega_o)\frac{\delta A}{A_o} + |\,Z'(\omega_o)\,|^2\frac{1}{A_o}\frac{d\,\delta A}{dt} = 0.$$

If δA decays with time, we have

$$sR_oX'(\omega_o) - rR_oR'(\omega_o) > 0. \tag{12}$$

An operating point determined by equation (10) is stable if and only if it satisfies condition (12).

III. CONDITIONS FOR INJECTION LOCKING

Let us next investigate injection locking of the oscillator. The injection signal is represented by

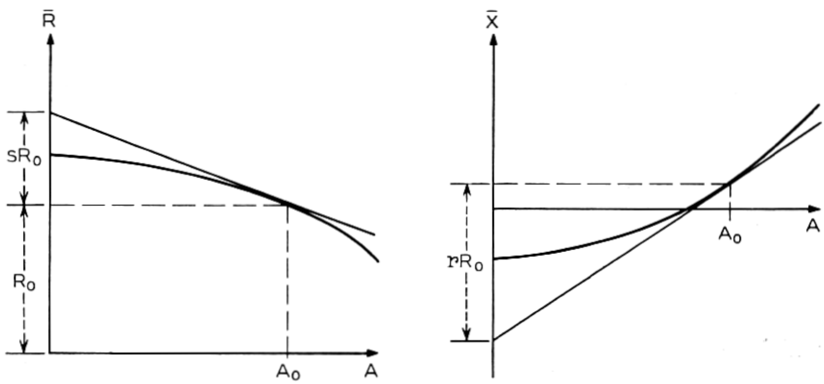

Fig. 3 — $\bar{R}$ versus A; $\bar{X}$ versus A.

$$e(t) = a_o \cos \omega_i t.$$

Then, from (6) and (7), we have

$$e_c(t) = a_o \cos \varphi, \quad e_s(t) = a_o \sin \varphi. \tag{13}$$

Since ω_i may differ from ω_o, and A from A_o, we write

$$R(\omega_i) - \bar{R} = \frac{\Delta A}{A_o} sR_o + \Delta R, \qquad X(\omega_i) + \bar{X} = \frac{\Delta A}{A_o} rR_o + \Delta X \tag{14}$$

where $\Delta R = R(\omega_i) - R(\omega_o)$ and $\Delta X = X(\omega_i) - X(\omega_o)$. Substituting (13) and (14) into (8) and (9) gives

$$\left(\frac{\Delta A}{A_o} sR_o + \Delta R\right) X'(\omega_i) - \left(\frac{\Delta A}{A_o} rR_o + \Delta X\right) R'(\omega_i) + | Z'(\omega_i) |^2 \frac{1}{A_o} \frac{d\,\Delta A}{dt} = \frac{a_o}{A_o} \{X'(\omega_i) \cos \varphi + R'(\omega_i) \sin \varphi\} \tag{15}$$

$$\left(\frac{\Delta A}{A_o} sR_o + \Delta R\right) R'(\omega_i) + \left(\frac{\Delta A}{A_o} rR_o + \Delta X\right) X'(\omega_i) + | Z'(\omega_i) |^2 \frac{d\varphi}{dt} = \frac{a_o}{A_o} \{R'(\omega_i) \cos \varphi - X'(\omega_i) \sin \varphi\}. \tag{16}$$

When the oscillator is locked $d\,\Delta A/dt = 0$, $d\varphi/dt = 0$. Substituting these conditions into (15) and (16) and eliminating ΔA we have

$$\frac{a_o}{A_o} (s^2 + r^2)^{\frac{1}{2}} \sin (\varphi_o + \theta) = r\,\Delta R - s\,\Delta X \tag{17}$$

where φ_o is the phase of the steady-state current and θ is defined by

$$\tan \theta = r/s. \tag{18}$$

Since the magnitude of $\sin(\varphi_o + \theta)$ must be less than one, (17) leads to the condition

$$\frac{A_o}{a_o} \frac{| r\,\Delta R - s\,\Delta X |}{(s^2 + r^2)^{\frac{1}{2}}} \leqq 1 \tag{19}$$

which determines the possible locking range.

Next, assume that ΔA and φ deviate from the steady-state values ΔA_o and φ_o and write $\Delta A = \Delta A_o + \delta A$ and $\varphi = \varphi_o + \delta\varphi$. Then, (15) and (16) become

$$\frac{\delta A}{A_o}[sR_oX'(\omega_i) - rR_oR'(\omega_i)] + |Z'(\omega_i)|^2 \frac{1}{A_o}\frac{d\,\delta A}{dt}$$

$$= \frac{a_o}{A_o}[-X'(\omega_i)\sin\varphi_o + R'(\omega_i)\cos\varphi_o]\,\delta\varphi \qquad (20)$$

$$\frac{\delta A}{A_o}[sR_oR'(\omega_i) + rR_oX'(\omega_i)] + |Z'(\omega_i)|^2 \frac{d\,\delta\varphi}{dt}$$

$$= \frac{a_o}{A_o}[-R'(\omega_i)\sin\varphi_o - X'(\omega_i)\cos\varphi_o]\,\delta\varphi. \qquad (21)$$

Eliminating δA from equations (20) and (21) gives

$$|Z'(\omega_i)|^2 \frac{d^2\,\delta\varphi}{dt^2} + \Big\{sR_oX'(\omega_i) - rR_oR'(\omega_i)$$

$$+ \frac{a_o}{A_o}[R'(\omega_i)\sin\varphi_o + X'(\omega_i)\cos\varphi_o]\Big\}\frac{d\,\delta\varphi}{dt}$$

$$+ \frac{a_o}{A_o}R_o(s^2 + r^2)^{\frac{1}{2}}\cos(\varphi_o + \theta)\,\delta\varphi = 0.$$

For stable operation, $|\delta\varphi|$ must decrease with time if it is not already zero. Thus, we have two conditions

$$sR_oX'(\omega_i) - rR_oR'(\omega_i) + \frac{a_o}{A_o}[R'(\omega_i)\sin\varphi_o + X'(\omega_i)\cos\varphi_o] > 0$$

$$\frac{a_o}{A_o}R_o(s^2 + r^2)^{\frac{1}{2}}\cos(\varphi_o + \theta) > 0. \qquad (22)$$

The first is usually satisfied if $sR_oX'(\omega_i) - rR_oR'(\omega_i)$ is positive, as required for a stable free-running oscillation at ω_i (not ω_o). The second condition is equivalent to

$$\cos(\varphi_o + \theta) > 0. \qquad (23)$$

The term φ_o is uniquely determined from equations (17) and (23). Using this φ_o, the left-hand side of equation (22) must then be calculated to check whether or not the locking is stable.

The above discussion was in terms of voltage and current. Since power is a more meaningful quantity at microwave frequencies, let us rewrite equations (17), (19), and (22). For simplicity, we assume that the box in Fig. 1 is lossless. Since the available power is invariant under a lossless transformation the injected signal power P_i is given by

$$P_i = \frac{a_o^2}{8(R_o + \triangle R)}.$$

The free-running output power is equal to

$$P_o = R_o \frac{A_o^2}{2}.$$

Using the above relations, equation (17) can be rewritten as

$$\triangle R \sin \theta - \triangle X \cos \theta \cong 2R_o(P_i/P_o)^{\frac{1}{2}} \sin (\varphi_o + \theta) \tag{24}$$

where higher order terms of $\triangle R$ are neglected. The locking range is determined from

$$| \triangle R \sin \theta - \triangle X \cos \theta | \leqq 2R_o(P_i/P_o)^{\frac{1}{2}} \tag{25}$$

$$(s^2 + r^2)^{\frac{1}{2}} R_o \sin (\Theta - \theta) + 2R_o(P_i/P_o)^{\frac{1}{2}} \sin (\Theta + \varphi_o) > 0 \tag{26}$$

where

$$\tan \Theta = \frac{X'(\omega_i)}{R'(\omega_i)}. \tag{27}$$

Equations (25) and (26) correspond to equations (19) and (22), respectively. To the same order of approximation, the output power of the locked oscillator is given by

$$\begin{aligned} P = P_o \Bigg\{ 1 + \frac{\triangle R}{R_o} - \frac{2}{R_o} \frac{\triangle R X'(\omega_i) - \triangle X R'(\omega_i)}{sX'(\omega_i) - rR'(\omega_i)} \\ + 4\left(\frac{P_i}{P_o}\right)^{\frac{1}{2}} \left[\frac{X'(\omega_i) \cos \varphi_o + R'(\omega_i) \sin \varphi_o}{sX'(\omega_i) - rR'(\omega_i)} - \tfrac{1}{2} \cos \varphi_o \right] \Bigg\} \end{aligned} \tag{28}$$

where the power wave concept has been used in the calculation.[9]

IV. NOISE AND PARASITIC OSCILLATIONS

Oscillator noise near the carrier can be discussed in terms of fluctuations in A and φ, just as in a single-tuned oscillator. Let $e(t)$ indicate a noise voltage in equations (6) and (7); then we have (see Ref. 5)

$$e_c(t) = n_1(t), \quad e_s(t) = n_2(t)$$

where $n_1(t)$ and $n_2(t)$ represent the cosine and sine components of the noise voltage $e(t)$ and

$$\overline{n_1(t)^2} = \overline{2e(t)^2}, \qquad \overline{n_2(t)^2} = \overline{2e(t)^2}, \qquad \overline{n_1(t)n_2(t)} = 0.$$

Substituting the above expressions into equations (8) and (9), we obtain

$$sR_oX'(\omega_o)\ \delta A - rR_oR'(\omega_o)\ \delta A + |\ Z'(\omega_o)\ |^2 \frac{d\ \delta A}{dt}$$

$$= X'(\omega_o)n_1(t) + R'(\omega_o)n_2(t)$$

$$sR_oR'(\omega_o)\ \delta A + rR_oX'(\omega_o)\ \delta A + |\ Z'(\omega_o)\ |^2\ A_o \frac{d\varphi}{dt}$$

$$= R'(\omega_o)n_1(t) - X'(\omega_o)n_2(t)$$

from which the frequency spectra of δA and φ are calculated as

$$|\ \delta A(f)\ |^2 = \frac{2\ |\ Z'(\omega_o)\ |^2\ |\ e\ |^2}{\omega^2\ |\ Z'(\omega_o)\ |^4 + [sR_oX'(\omega_o) - rR_oR'(\omega_o)]^2} \tag{29}$$

$$|\ \varphi(f)\ |^2 = \frac{2\ |\ e\ |^2}{\omega^2 A_o^2}\ \frac{\omega^2\ |\ Z'(\omega_o)\ |^2 + (s^2 + r^2)R_o^2}{\omega^2\ |\ Z'(\omega_o)\ |^4 + [sR_oX'(\omega_o) - rR_oR'(\omega_o)]^2}. \tag{30}$$

These equations indicate that the oscillation becomes very noisy as we approach the boundary of the stable region defined by equation (12). This is what we expect. However, equation (29) and (30) are not valid near the boundary since δA is no longer small, as was initially assumed.

Sometimes we need to consider additional current components at frequencies $\omega \pm \Delta\omega$, so far away from the oscillating frequency ω that, although $\Delta\omega \ll \omega$, equation (3) is no longer a valid approximation. In this case, we express the current in the form

$$i(t) = A \cos (\omega t + \varphi) + A_+ \cos \{(\omega + \Delta\omega)t + \varphi_+\}$$

$$+ A_- \cos \{\omega - \Delta\omega)t + \varphi_-\} \tag{31}$$

where A, φ, A_+, φ_+ A_-, and φ_- are all slowly varying functions of time. Assuming that $A_+ \ll A$ and $A_- \ll A$, and neglecting higher order terms of small quantities, the current can be expressed as

$$i(t) = \tilde{A} \cos (\omega t + \tilde{\varphi})$$

where

$$\tilde{A} = A + A_+ \cos (\Delta\omega t + \varphi_+ - \varphi) + A_- \cos (\Delta\omega t - \varphi_- + \varphi)$$

$$\tilde{\varphi} = \varphi + \frac{1}{A} \{A_+ \sin (\Delta\omega t + \varphi_+ - \varphi) - A_- \sin (\Delta\omega t - \varphi_- + \varphi)\}.$$

The voltage drop across the active device is then given by

$$
\begin{aligned}
v &= -\bar{R}(\tilde{A})\tilde{A} \cos(\omega t + \tilde{\varphi}) - \bar{X}(\tilde{A})\tilde{A} \sin(\omega t + \tilde{\varphi}) \\
&\cong -\bar{R}A \cos(\omega t + \varphi) - \bar{X}A \sin(\omega t + \varphi) \\
&\qquad - \left(2\bar{R} + \frac{\partial \bar{R}}{\partial A} A\right) \frac{A_+}{2} \cos[(\omega + \Delta\omega)t + \varphi_+] \\
&\qquad - \frac{\partial \bar{R}}{\partial A} A \frac{A_-}{2} \cos[(\omega + \Delta\omega)t + 2\varphi - \varphi_-] \\
&\qquad - \left(2\bar{X} + \frac{\partial \bar{X}}{\partial A} A\right) \frac{A_+}{2} \sin[(\omega + \Delta\omega)t + \varphi_+] \\
&\qquad - \frac{\partial \bar{X}}{\partial A} A \frac{A_-}{2} \sin[(\omega + \Delta\omega)t + 2\varphi - \varphi_-] \\
&\qquad - \left(2\bar{R} + \frac{\partial \bar{R}}{\partial A} A\right) \frac{A_-}{2} \cos[(\omega - \Delta\omega)t + \varphi_-] \\
&\qquad - \frac{\partial \bar{R}}{\partial A} A \frac{A_+}{2} \cos[(\omega - \Delta\omega)t + 2\varphi - \varphi_+] \\
&\qquad - \left(2\bar{X} + \frac{\partial \bar{X}}{\partial A} A\right) \frac{A_-}{2} \sin[(\omega - \Delta\omega)t + \varphi_-] \\
&\qquad - \frac{\partial \bar{X}}{\partial A} A \frac{A_-}{2} \sin[(\omega - \Delta\omega)t + 2\varphi - \varphi_+] \qquad (32)
\end{aligned}
$$

where $\bar{R}$ and $\bar{X}$ express the values at A, that is, $\bar{R}(A)$ and $\bar{X}(A)$, respectively. To derive equation (32), an assumption was made that the values of $\bar{R}$ and $\bar{X}$ change with time following the envelope of the current, which is generally a valid assumption when $\Delta\omega \ll \omega$, as assumed here. The voltage drop across the impedance $Z(\omega)$ can be calculated as follows.

$$
\begin{aligned}
\mathrm{Re}\,\{ZI\} &= \left[AR(\omega) + AR'(\omega)\frac{d\varphi}{dt} + X'(\omega)\frac{dA}{dt}\right] \cos(\omega t + \varphi) \\
&\quad - \left[AX(\omega) + AX'(\omega)\frac{d\varphi}{dt} - R'(\omega)\frac{dA}{dt}\right] \sin(\omega t + \varphi) \\
&\quad + \left(A_+R_+ + A_+R'_+\frac{d\varphi_+}{dt} + X'_+\frac{dA_+}{dt}\right) \cos[(\omega + \Delta\omega)t + \varphi_+] \\
&\quad - \left(A_+X_+ + A_+X'_+\frac{d\varphi_+}{dt} - R'_+\frac{dA_+}{dt}\right) \sin[(\omega + \Delta\omega)t + \varphi_+]
\end{aligned}
$$

$$+\left(A_-R_- + A_-R'_-\frac{d\varphi_-}{dt} + X'_-\frac{dA_-}{dt}\right)\cos\left[(\omega - \Delta\omega)t + \varphi_-\right]$$

$$-\left(A_-X_- + A_-X'_-\frac{d\varphi_-}{dt} - R'_-\frac{dA_-}{dt}\right)\sin\left[(\omega - \Delta\omega)t + \varphi_-\right]$$

where $R_+ = R(\omega + \Delta\omega)$, $X_+ = X(\omega + \Delta\omega)$, $R_- = R(\omega - \Delta\omega)$ and $X_- = X(\omega - \Delta\omega)$.

Let n be defined by $2\pi/T_o\Delta\omega$. Multiplying Re $\{ZI\} + v = e(t)$ by $\cos(\omega t + \varphi)$ and $\sin(\omega t + \varphi)$, and integrating the results over a period of nT_o, we obtain approximate equations for A and φ. These are identical to equations (4) and (5), except that $e_c(t)$ and $e_s(t)$ are now defined by

$$e_c(t) = \frac{2}{nT_o}\int_{t-nT_o}^{t} e(t)\cos(\omega t + \varphi)\,dt,$$

$$e_s(t) = \frac{2}{nT_o}\int_{t-nT_o}^{t} e(t)\sin(\omega t + \varphi)\,dt.$$

This means that A and φ of free running and of injection-locked oscillators behave exactly in the same manner. For example, the amplitude of the free-running oscillation is determined by equation (10) and hence $(\partial\bar{R}/\partial A)A$ and $(\partial\bar{X}/\partial A)A$ in equation (32) can be replaced by $-sR_o$ and rR_o, respectively. The integration of Re $\{ZI\} + v = e(t)$ over a period of nT_o after multiplying by $\cos[(\omega + \Delta\omega)t + \varphi_+]$, and so on, gives

$$\begin{aligned}(R_+ - \bar{R} + \tfrac{1}{2}sR_o)A_+ + R'_+A_+\frac{d\varphi_+}{dt} + X'_+\frac{dA_+}{dt}& \\ + (sR_o\cos\delta - rR_o\sin\delta)\frac{A_-}{2}& \\ = \frac{2}{nT_o}\int_{t-nT_o}^{t} e(t)\cos\{(\omega + \Delta\omega)t + \varphi_+\}\,dt,&\end{aligned} \tag{33}$$

$$\begin{aligned}-(X_+ + \bar{X} + \tfrac{1}{2}rR_o)A_+ - X'_+A_+\frac{d\varphi_+}{dt} + R'_+\frac{dA_+}{dt}& \\ - (rR_o\cos\delta + sR_o\sin\delta)\frac{A_-}{2}& \\ = \frac{2}{nT_o}\int_{t-nT_o}^{t} e(t)\sin\{(\omega + \Delta\omega)t + \varphi_+\}\,dt&\end{aligned} \tag{34}$$

and two similar equations, in which the subscripts $+$ and $-$ are interchanged and $+\Delta\omega$ is replaced by $-\Delta\omega$. These are the basic equations determining the behavior of A_+, A_-, φ_+, and φ_-. In equations (33) and (34), δ stands for $2\varphi - \varphi_- - \varphi_+$.

When $e(t)$ equals zero, the above equations usually give $A_+ = A_- = 0$. However, if the condition

$$\frac{R_+ - \bar{R} + \frac{1}{2}sR_o}{X_+ + \bar{X} + \frac{1}{2}rR_o} = \frac{R_- - \bar{R} + \frac{1}{2}sR_o}{X_- + \bar{X} + \frac{1}{2}rR_o} \tag{35}$$

is satisfied, the steady-state values of A_+ and A_- can become finite even when the integrals in equations (33), and (34) (and the other two equations) are all zero. Condition (35) is not satisfied by a single-tuned oscillator. With a multiple-resonant circuit, however, the locus of $Z(\omega)$ on the complex plane may form a loop (or loops) which intersects with itself; the above condition is often satisfied at a certain oscillation frequency (or frequencies). This means that as the oscillation frequency approaches this particular value the noise output power at $\omega \pm \Delta\omega$ increases enormously, resulting in a noisy parasitic oscillation; this first-order discussion then becomes invalid.

The noise of locked oscillators with a multiple-resonant circuit can be treated in a way similar to that of a single-tuned locked oscillator. For simplicity, let us assume that the locking signal is noise-free. Then, we have

$$\begin{aligned} |\delta A|^2 = {} & [(\omega^2 A^2 |Z'|^2 + a_o^2)2 |e|^2] \\ & \cdot \{[\omega^2 A |Z'|^2 - a_o(sR_o \cos\varphi_o - rR_o \sin\varphi_o)]^2 \\ & + \omega^2[A(sR_oX' - rR_oR') + a_o(R' \sin\varphi_o + X' \cos\varphi_o)]^2\}^{-1} \end{aligned} \tag{36}$$

$$\begin{aligned} |\delta\varphi|^2 = {} & \{[\omega^2 |Z'|^2 + (s^2 + r^2)R_o^2]2 |e|^2\} \\ & \cdot \{[\omega^2 A |Z'|^2 - a_o(sR_o \cos\varphi_o - rR_o \sin\varphi_o)]^2 \\ & + \omega^2[A(sR_oX' - rR_oR') + a_o(R' \sin\varphi_o + X' \cos\varphi_o)]^2\}^{-1} \end{aligned} \tag{37}$$

where Z', R' and X' indicate their values at ω_i.

The parasitic oscillations also take place in the injection-locked oscillators at the same frequency as before. This is because the injection-locked signal does not contribute to the values of the integrals in equation (33), and the condition for parasitic oscillations remains the same.

V. GRAPHICAL INTERPRETATION

An excellent discussion of oscillator behaviors using a graphical method was already presented by Slater in his book *Microwave Elec-*

tronics. This section will extend his method first by including the case in which the locus of $Z(\omega)$ forms a loop (or loops),* and then by discussing injection locking.

Suppose that the locus of $Z(\omega)$ and the line representing $\bar{R} - j\bar{X}$ are drawn on the complex plane as shown in Fig. 4. The parameters are ω and A; the arrows indicate the directions of increasing ω and A. According to equation (10), the intersections of these two curves give possible operating points. For intersection (a), $sR'(\omega) > 0$ and

$$R_o\left(\frac{X'(\omega)}{R'(\omega)} - \frac{r}{s}\right) = R_o(\tan \Theta - \tan \theta) > 0.$$

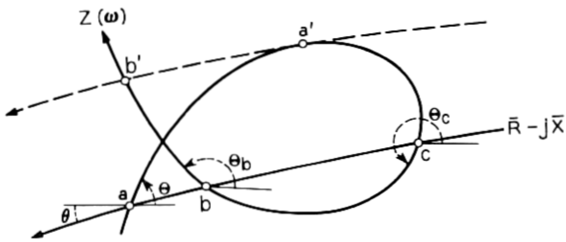

Fig. 4 — Z (ω) and $\bar{R} - j\bar{X}$ on the complex plane.

From equation (12), (a) is a stable operating point. For intersection (b), $sR'(\omega) < 0$ and hence equation (12) becomes

$$R_0\left(\frac{X'(\omega)}{R'(\omega)} - \frac{r}{s}\right) = R_o(\tan \Theta - \tan \theta) < 0.$$

This inequality is satisfied and intersection (b) represents another stable operating point. However, intersection (c) is unstable since $sR'(\omega) < 0$ and $\tan \Theta - \tan \theta > 0$.

Which of the two stable operating points the oscillation selects depends on the oscillation's history. Suppose an oscillation corresponding to (a) is taking place and $\bar{X}$ is gradually decreased, then the curve $\bar{R} - j\bar{X}$ moves up and the intersection (a) moves toward the right until it reaches (a'). If we further decrease $\bar{X}$ the intersection (a') disappears and the operating point jumps to (b'). Just before it jumps the oscillation becomes very noisy [since

$$sR_oX'(\omega) - rR_oR'(\omega) = (s^2 + r^2)^{\frac{1}{2}}R_o \mid Z'(\omega) \mid \sin (\Theta - \theta)$$

in the denominator of the noise expression (29) becomes zero and

* In this case $\omega = \omega_1 + j\omega_2$ becomes a multivalued function of impedance.

$|\ \delta A(f)\ |$ becomes infinite as $\omega \to 0$]. After the jump, if $\bar{X}$ is increased to its original value, operating point (b) is reached. Similarly, with the operating point initially at (b) we can realize operating point (a) by increasing $\bar{X}$ sufficiently and then bringing it back to the original value. If $\bar{X}$ cannot be changed, we might still be able to change the circuit so as to move the locus of $Z(\omega)$ up or down, thereby producing the same effect. During these adjustments, if three points $\bar{R} - \frac{1}{2}sR_o - j(\bar{X} + \frac{1}{2}rR_o)$, $R_+ + jX_+$, and $R_- + jX_-$ happen to fall on a straight line as illustrated in Fig. 5, then condition (35) is satisfied and we observe simultaneous oscillations at three different frequencies (sometimes more than three at $\omega \pm m\triangle\omega$, with m representing integers).

Let us next consider the injection locking case. Suppose that the free-running operating point is at (a) in Fig. 6. In order to lock the oscillator at ω corresponding to point (e) in Fig. 6, the conditions for stable locking, equations (25) and (26), must be satisfied. Since $|\ \triangle R \sin \theta - \triangle X \cos \theta\ |$ corresponds to the distance from (e) to the line $\bar{R} - j\bar{X}$ as illustrated in Fig. 6a, we see that if this distance is less than $2R_o \cdot (P_o/P_o)^{\frac{1}{2}}$ the first condition is satisfied. Then, from equations (23) and (24) φ can be graphically obtained as shown in Fig. 6b. In this particular case φ is negative, but when (e) is located sufficiently below (a), φ becomes positive. Using this φ, $2R_o(P_i/P_o)^{\frac{1}{2}} \sin(\Theta + \varphi)$ can be evaluated; for example, as shown in Fig. 6c, and if condition (26) is satisfied, (e) is in the stable locking range. This condition is generally satisfied when $P_i \ll P_o$, unless (e) is located near the boundary point of the stable free-running oscillation such as (a') in Fig. 4. (Notice that s is equal to 2 if the circuit is adjusted for maximum power.)

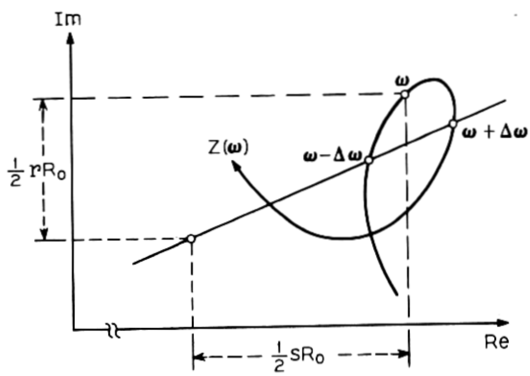

Fig. 5 — Condition for parasitic oscillations.

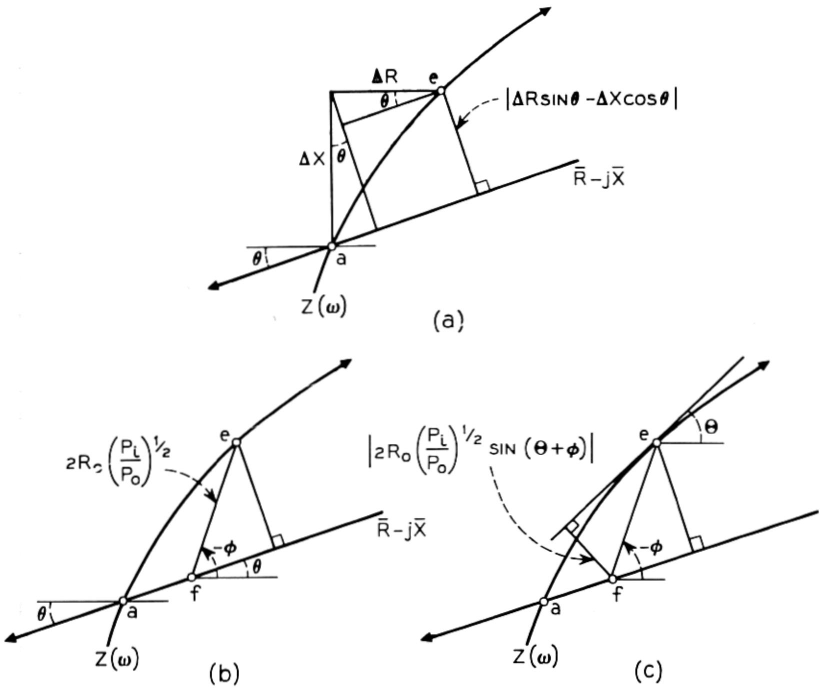

Fig. 6 — Graphical explanation of locking conditions.

The apparent impedance presented to the active device is given by

$$Z(\omega) - \frac{E}{I} = Z(\omega) - \frac{a_o e^{j\omega t}}{Ae^{i(\omega t+\varphi)}} = Z(\omega) - 2R_o(P_i/P_o)^{\frac{1}{2}}e^{-i\varphi}$$

where E and I are the complex representations of $e(t)$ and $i(t)$, respectively. The last term on the right, including the minus sign, corresponds to a vector drawn from (e) to (f) in Fig. 6b. Consequently, the effect of the injection signal can be considered as that of adding to $Z(\omega)$ an impedance corresponding to this vector; the active device is operating at (f). This can be confirmed by calculating the amplitude of the oscillating current from equations (20) and (21) under steady-state conditions.

VI. BROADBAND OSCILLATOR CIRCUITS

Let us consider the frequency deviator. The oscillating frequency can be deviated by changing $\bar{X}$ of the active device, which may be a function of supply voltage or current. For an oscillator with a single-resonant circuit, the relative frequency deviation is given by

$$\frac{\Delta f}{f} = \frac{-1}{2Q_{\text{ext}}} \frac{\Delta \bar{X}}{\bar{R}} \tag{38}$$

where $\Delta \bar{X}$ indicates the variation in $\bar{X}$. In order to increase the magnitude of the frequency deviation for a given $\Delta \bar{X}/\bar{R}$, the external Q of the circuit, Q_{ext}, must be reduced. However, it cannot be made smaller than the Q of the active device, and in practice it tends to be larger by as much as an order of magnitude because of the difficulty in obtaining strictly lumped-constant elements at microwave frequencies.

Suppose that everything has been done to reduce Q_{ext} to its practical limit; the next thing to consider is the possibility of adding another resonant circuit as shown in Fig. 7. The series arm of L_1 and C_1 represents the original resonant circuit; the parallel resonant circuit L_2, C_2 has been added. For simplicity, let us assume

$$\omega_0 = (L_1C_1)^{-\frac{1}{2}} = (L_2C_2)^{-\frac{1}{2}}.$$

The locus of the impedance $Z(\omega)$, looking from the active device, should then look like Fig. 8, depending on the relative magnitude of the Q's of the resonant circuits (which are defined by $Q_1 = \omega_o L_1/R_L = Q_{\text{ext}}$, $Q_2 = \omega_o C_2 R_L$). The markers indicate equally spaced frequencies. Figure 8a shows the limiting case of $L_2 \to \infty$ and $C_2 \to 0$, which corresponds to the original single-tuned oscillator. From Section IV, it is now obvious how the oscillator behaves in each case. Thus, the conditions of Figs. 8c and d are to be avoided if smooth frequency deviation is desired. Consequently, we should concentrate on the case where $Q_2 < Q_1$. In the vicinity of the operating point shown in Fig. 8b,

$$X(\omega) \cong R_L(Q_1 - Q_2) \frac{2\,\Delta\omega}{\omega_o} \tag{39}$$

where $\Delta\omega = \omega - \omega_o$, so that the frequency deviation corresponding to a

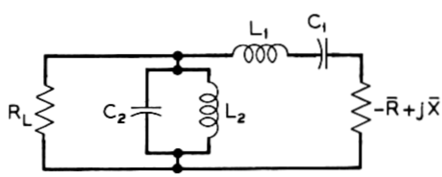

Fig. 7 — An oscillator with a double-resonant circuit.

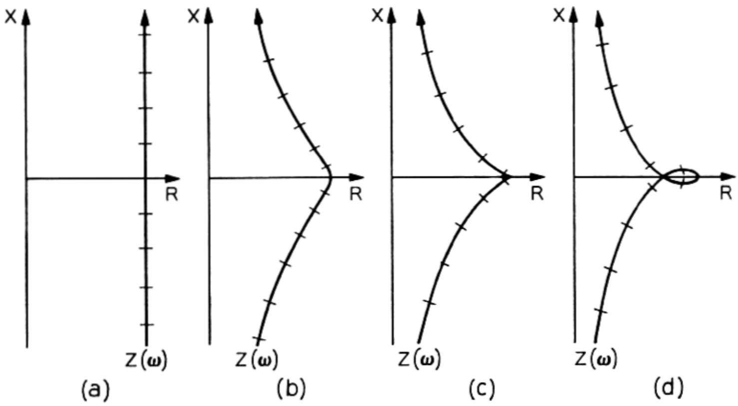

Fig. 8 — $Z(\omega)$ for the oscillator shown in Fig. 7.

small $\triangle\bar{X}$ is given by

$$\frac{\triangle f}{f} \cong \frac{1}{2(Q_1 - Q_2)} \frac{\triangle \bar{X}}{\bar{R}}. \tag{40}$$

As Q_2 approaches Q_1, $\triangle f/f$ increases for a given small $\triangle\bar{X}/\bar{R}$.

However, there are several disadvantages in bringing Q_2 too close to Q_1. The first is noise: since $R'(\omega_o) = 0$ and $X'(\omega_o)$ becomes small, from equation (30) the oscillator output becomes noisy. The second is nonlinearity: unless $Q_2(2\triangle\omega/\omega_o) \ll 1$, equation (39) and hence (40) become poor approximations. In fact, the frequency markers will be crowded near ω_o; they rapidly get sparser away from it. This means that the relation $\triangle f$ versus $\triangle\bar{X}$ is highly nonlinear, which is objectionable in certain applications. Finally, the output power $\frac{1}{2}\bar{R}A^2$ may change rapidly as we deviate from ω_o. This is because the intersection between $\bar{R} - j\bar{X}$ and $Z(\omega)$ moves to the left; hence, both A and $\bar{R}$ change. If the operating point is selected to maximize the output power, then the increase in A and the decrease in $\bar{R}$ may compensate for each other to produce approximately the same output power over a wide range of deviation, which is, however, highly dependent on the saturation characteristic of the device itself.

If the double-resonant circuit does not offer a satisfactory result because of its nonlinearity or power variation, one should consider triple or even higher order resonant circuits. If all the resonant circuits in the ladder structure shown in Fig. 9 are tuned to the same frequency ω_o, and if the Q's of the circuits satisfy

$$Q_1 + Q_2 + Q_4 + \cdots > Q_1 + Q_3 + \cdots > Q_2 + Q_4 + \cdots ,$$

then a broadbanding effect can be obtained near ω_o. However, the rate of return diminishes as we increase the complexity of the circuit.

Let us next consider injection locking of oscillators. It is clear from the discussion in Section IV that the circuits corresponding to Figs. 8c and d are not suitable. We, therefore, concentrate on Figs. 8a and b. The total locking range Δf can be calculated from

$$\frac{\Delta f}{f} = \frac{2}{Q_{\text{ext}}} \left(\frac{P_i}{P_o}\right)^{\frac{1}{2}} \frac{1}{\cos\theta}$$

$$\frac{\Delta f}{f} = \frac{2}{Q_1 - Q_2} \left(\frac{P_i}{P_o}\right)^{\frac{1}{2}} \frac{1}{\cos\theta}$$

for a single-resonant and a double-resonant oscillator, respectively. As Q_2 approaches Q_1, the locking range increases for given $(P_i/P_o)^{\frac{1}{2}}$. However, the output becomes noisy if we bring Q_2 too close to Q_1. Thus, some compromise must be made.

If a precise limiter action is desired, equation (28) should be closely investigated. If good linearity of φ versus $\Delta\omega$ is desired, multiple-resonant circuits are worth investigating. In any case, once the desired characteristic is given, it determines the necessary locus of $Z(\omega)$. Then, well-known techniques developed in connection with the design of filters are available to optimize the circuit parameters until the desired locus is sufficiently approximated.

In the above discussions, impedances were used exclusively. The same discussions can be carried out using admittances, producing no new results. However, when the active device has a large parallel capacitance, using admittances may have certain practical advantages since the capacitance can be more easily included in the multiple resonant circuit.

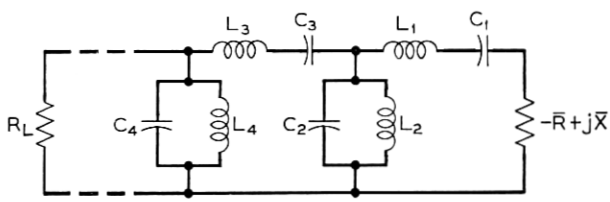

Fig. 9 — An oscillator with a multiple-resonant circuit.

VII. CONCLUSION

We have discussed, in detail, the expected behavior of negative resistance oscillators with multiple-resonant circuits. The systematic realization of microwave hardware which simulates these equivalent circuits still remains a problem for the future. Also, an accurate method to evaluate the device impedance $-\bar{R} + j\bar{X}$ must be developed before this discussion becomes more than just a guidance. Efforts in these directions are presently undertaken.

VIII. ACKNOWLEDGEMENT

Although they are not coauthors, N. D. Kenyon and J. P. Beccone contributed experimental investigations which were indispensable for developing the ideas presented here. Acknowledgment is due to R. S. Engelbrecht for his support, encouragement, and comments.

REFERENCES

1. Huntoon, R. D., and Weiss, A., "Synchronization of Oscillators," Proc. IRE, *35,* No. 12 (December 1947), pp. 1415–1423.
2. Hubbard, W. M., and others, "A Solid-State Regenerative Repeater for Guided Millimeter-Wave Communication Systems," B.S.T.J., *46,* No. 9 (November 1967), pp. 1977–2018.
3. Amoss, J. W., and Gsteiger, K. E., "Frequency Modulation of Avalanche Transit Time Oscillators," IEEE Trans., *MTT-15,* No. 12 (December 1967), pp. 742–747.
4. Ruthroff, C. L., "Injection-Locked-Oscillator FM Receiver Analysis," B.S.T.J., *47,* No. 8 (October 1968), pp. 1655–1661.
5. Minorsky, N., *Nonlinear Oscillators,* Princeton, N. J.: Van Nostrand, 1962.
6. Stoker, J. J., *Nonlinear Vibration,* New York: John Wiley, 1950.
7. Krylov, N., and Bogoliubov, N., *Introduction to Nonlinear Mechanics,* Princeton, N. J.: Princeton University Press, 1943.
8. Kurokawa, K., "Noise in Synchronized Oscillators," IEEE Trans., *MTT-16,* No. 4 (April 1968), pp. 234–240.
9. Kurokawa, K., "Power Waves and the Scattering Matrix," IEEE Trans., *MTT-13,* No. 2 (March 1965), pp. 194–202.

Note added in proof:

Since the submission of this article, the following book has been published. It discusses the power wave concept in detail. Also, chapter 9 is devoted to discussing oscillators with a single tuned circuit.

Kurokawa, K., *An Introduction to the Theory of Microwave Circuits,* New York: Academic Press, 1969.